Electronic Supplementary Material (ESI) for ChemComm.

Supplementary Information

for

Intramolecular catalysis, H-bonding and intramolecular proton dynamics affects the CEST properties of Eu^{III} complexes of HP-DO3A-like ligands

Simona Baroni,[a] Irene Maria Carnovale,[b] Carla Carrera,[c] Mariangela Boccalon,[d] Nicol Guidolin,[d] Nicola Demitri,[e] Luciano Lattuada,[d] Fabio Tedoldi,[d] Zsolt Baranyai[d,] Silvio Aime[a,*]*

[a] Department of Molecular Biotechnologies and Health Sciences, Molecular Imaging Center, University of Torino, Via Nizza 52, 10126 Torino, Italy.

[b] Department of Drug Science and Technology, University of Torino, Via. P. Giuria 7, 10125 Torino, Italy.

[c] Institute of Biostructures and Bioimaging, National Research Council, Via Nizza 52, 10126 Torino, Italy

[d] Bracco Imaging Spa, Bracco Research Centre, Via Ribes 5, 10010 Colleretto Giacosa (TO), Italy

[e] Elettra–Sincrotrone Trieste, S.S. 14 Km 163.5 in Area Science Park, Basovizza, 34149 Trieste, Italy

Content:

I. NMR studies of Eu(HP-DO3A) derivatives.

I.1. Materials and Methods

Materials: The chemicals used for the experiments were of the highest analytical grade. The synthesis of the An-HP-DO3A and Bz-HP-DO3A ligands and those of Gd^{III}-complexes were carried out as described in Ref. S1. The Eu^{III} complexes of HP-DO3A (*Bracco Imaging Spa*) and An-HP-DO3A were prepared by mixing stoichiometric amounts of ligand with the europium chloride hexahydrate in water. The pH of the solution was brought to 7 by addition of 1 M NaOH solution. The solution was stirred at room temperature for 16 h. In order to hydrolyze the lactone might be formed by the benzoate derivative, the aqueous solution of Bz-HP-DO3A at pH=12 was stirred for 18 h. The solution was heated at 40°C for 1 h then cooled to room temperature. The pH of solution was brought to 7 by addition of 37% HCl then stoichiometric amount of europium chloride hexahydrate was added and the solution stirred at room temperature for 16 h. The complexation process was monitored by high resolution NMR spectroscopy. Electrospray ionization time-of-flight mass spectrometry (ESI-TOF-MS) has been used for the detailed characterization of the Eu^{III}-complexes. ESI-TOF-MS measurements were performed with a MicrOTOF Focus (*Bruker Daltonics*) mass spectrometer equipped with an automatic syringe pump (*KD Scientific*) for sample injection. The ESI-TOF mass spectrometer was running at 4.5 kV at a desolvation temperature of 180 °C. The mass spectrometer was operating in the positive ion mode. The standard electrospray ion (ESI) source was used to generate the ions. The ESI-TOF-MS instrument was calibrated in the m/z range 50-3000 using an internal calibration standard (*Tunemix solution*) which is supplied by *Agilent*. Data were processed via *Bruker Data Analysis* software version 4.1. MS (ESI) m/z of Eu(HP-DO3A) calculated for $C_{17}EuH_{29}N_4O_7$ 577.11, found 577.13 $[M + Na]^+$. MS (ESI) m/z of Eu(An-HP-DO3A) calculated for $C_{22}EuH_{32}N_5O_7$ 654.14, found 654.18 $[M + Na]^+$. MS (ESI) m/z of Eu(Bz-HP-DO3A) calculated for $C_{23}EuH_{31}N_4O_9$ 705.10, found 705.15 $[M - H + 2Na]^+$.

^{1}H NMR spectroscopy: The spectra of the Eu^{III}-complexes were recorded by Bruker Avance III 400 (9.4 T) or 600 (14.1 T) NMR spectrometers equipped with BB inverse z gradient probe (5 mm). The temperature of the sample holder was kept constant with a thermostated air stream. Eu^{III} complex was dissolved in H_2O, D_2O, DMSO-d_6/H_2O and DMSO-d_6/D_2O mixtures (80/20 v/v%). The concentration of the Eu^{III}-complexes for NMR experiment was assessed by the Evans method.[S2] The pH was adjusted by addition of DCl or HCl and KOD or KOH solutions. For the pH measurements, *Metrohm 932* pH-meter and *Metrohm-6.0234.110* combined electrode were used. Samples were stirred with a magnetic stirrer and N_2 gas was bubbled through them. For the calibration of the pH meter, KH-phthalate ([KH-phthalate]=0.05 M, pH=4.002) and borax ([borax]=0.01 M, pH=9.177) buffers were used at 25°C.

CEST Experiments and Data Analysis: Z-spectra were acquired at 7 T on a Bruker Avance 300 spectrometer equipped with a microimaging probe and a 10 mm resonator. A frequency offset range of ± 100 ppm was investigated. A typical RARE spin–echo with a RARE factor of 32, an echo time of 3 ms and a TR value of 5 s was used. An isotropic 64 × 64 acquisition matrix with a FOV of 11 mm and a slice thickness of 1.5 mm were used. The whole sequence was preceded by a saturation scheme consisting of a continuous rectangular wave pulse 2 s long with a RF B_1 intensity ranging from 6 to12 μT.
Raw Z-spectra data were exported from the MRI workstation and automatically elaborated by means of software executed in MATLAB (The Mathworks Inc., Natick, MA, USA). The analysis consisted of several steps [image segmentation, global region of interest (ROI) analysis, local voxel-by-voxel analysis] according to our previously reported method. Z-spectra were interpolated by using smoothing splines.[S3,S4] The extent of CEST effect (ST %) was calculated as follows:

$$ST\% = \left(\frac{I^{OFF} - I^{ON}}{I^{OFF}} \right) \times 100 \qquad (S1)$$

where I^{ON} and I^{OFF} are the resonance frequency offset of the mobile protons of the CEST agent and the water intensity at the contralateral frequency, respectively.

I.2. ^{1}H-NMR spectra of the Eu^{III}-complexes

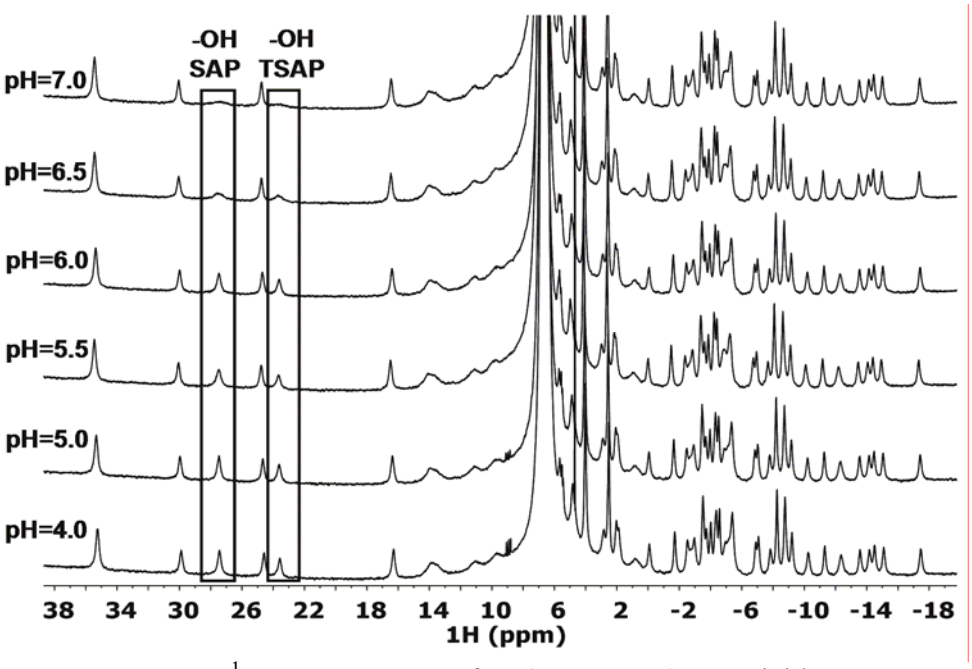

Figure S1. ^{1}H NMR spectra of Eu(HP-DO3A) at variable pH ([EuL]=0.1 M, 9.4 T, 293 K, 1.0 M NaCl)

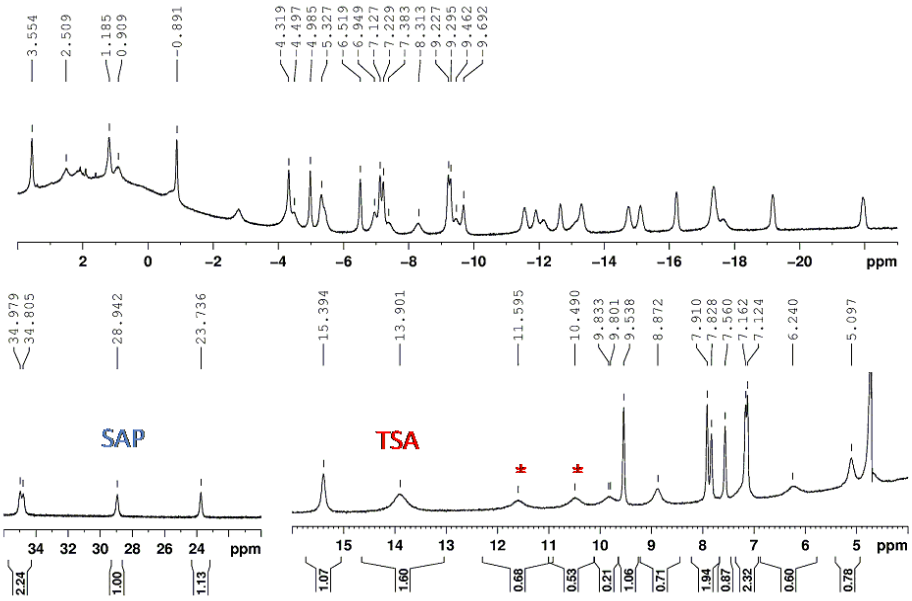

Figure S2. ^{1}H-NMR spectra of Eu(Bz-HP-DO3A) complex ([EuL]=2.5 mM, pD=7.7, 14.1 T, D_2O, 278 K)

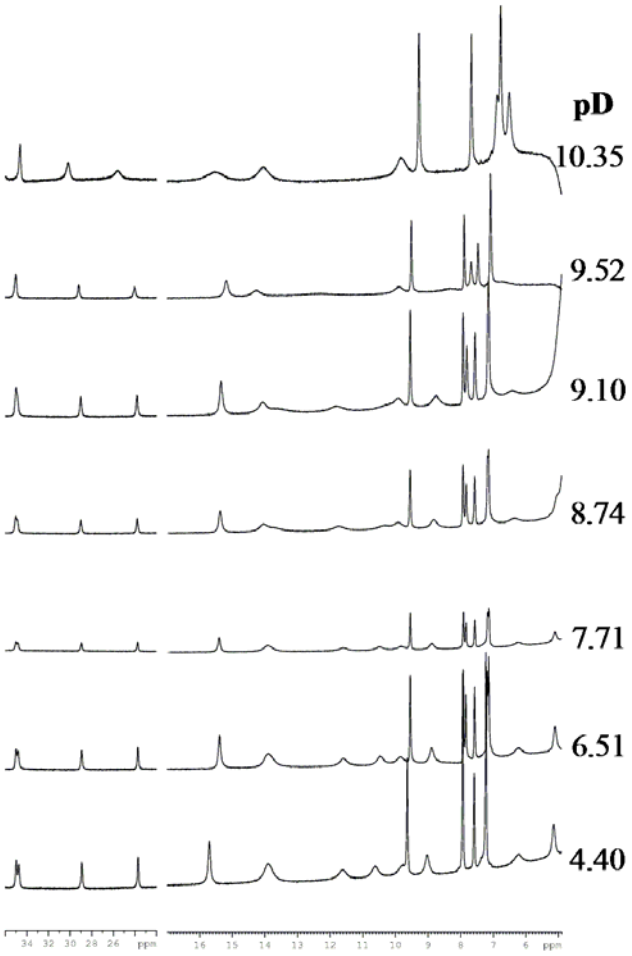

Figure S3. ^{1}H-NMR spectra of Eu(Bz-HP-DO3A) complex in the pD range 4.4 – 10.4 ([EuL]=2.5 mM, 14.1 T, D_2O, 278 K)

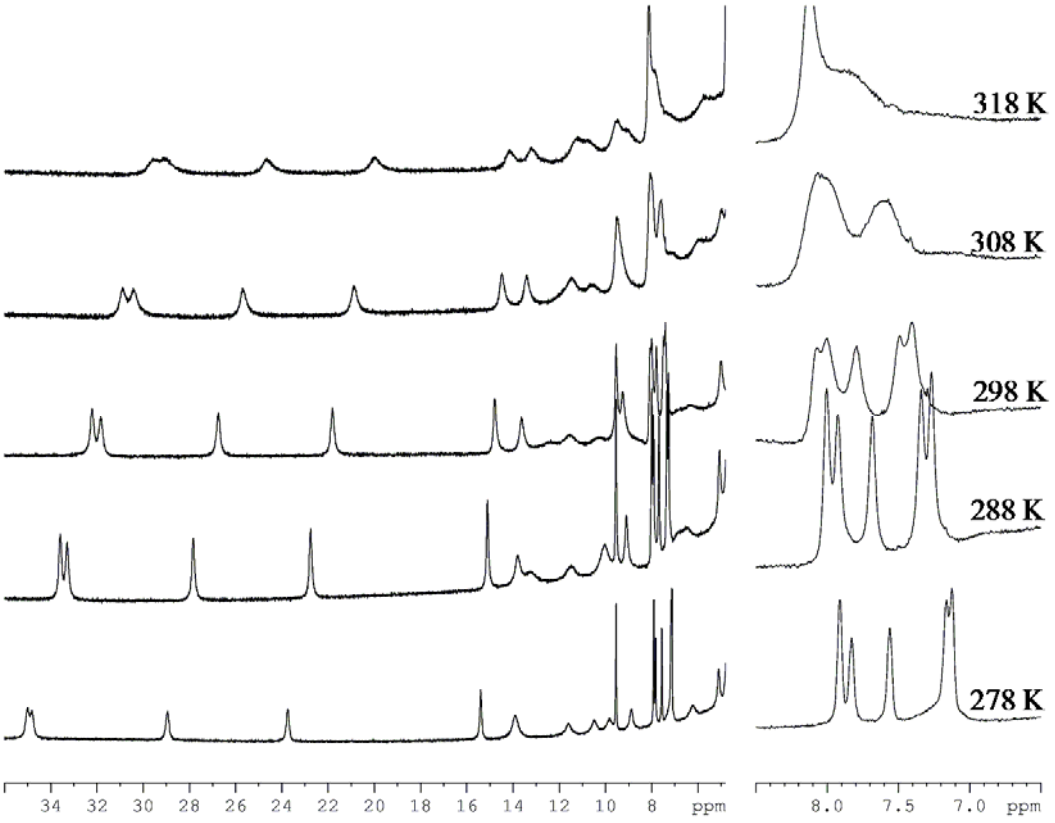

Figure S4. VT ^{1}H-NMR spectra of Eu(Bz-HP-DO3A) complex ([EuL]=2.5 mM, pD=7.7, 14.1 T, D_2O)

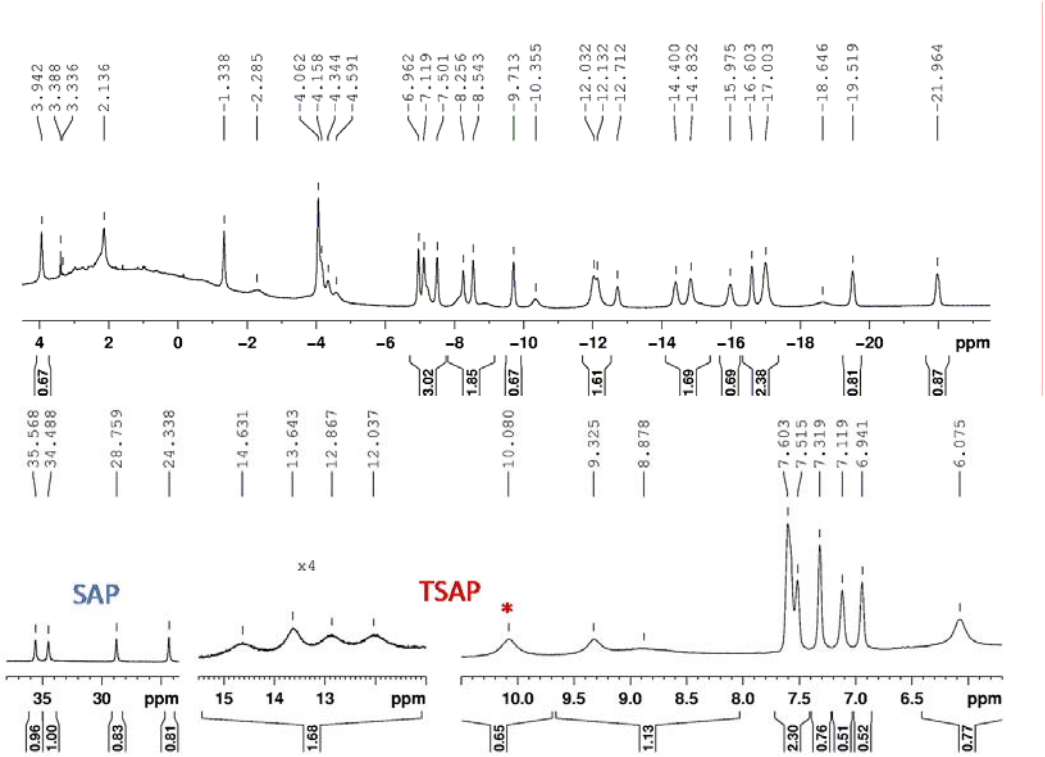

Figure S5. ^{1}H-NMR spectra of Eu(An-HP-DO3A) complex ([EuL]=2.0 mM, pD=7.68, 14.1 T, D_2O, 278 K)

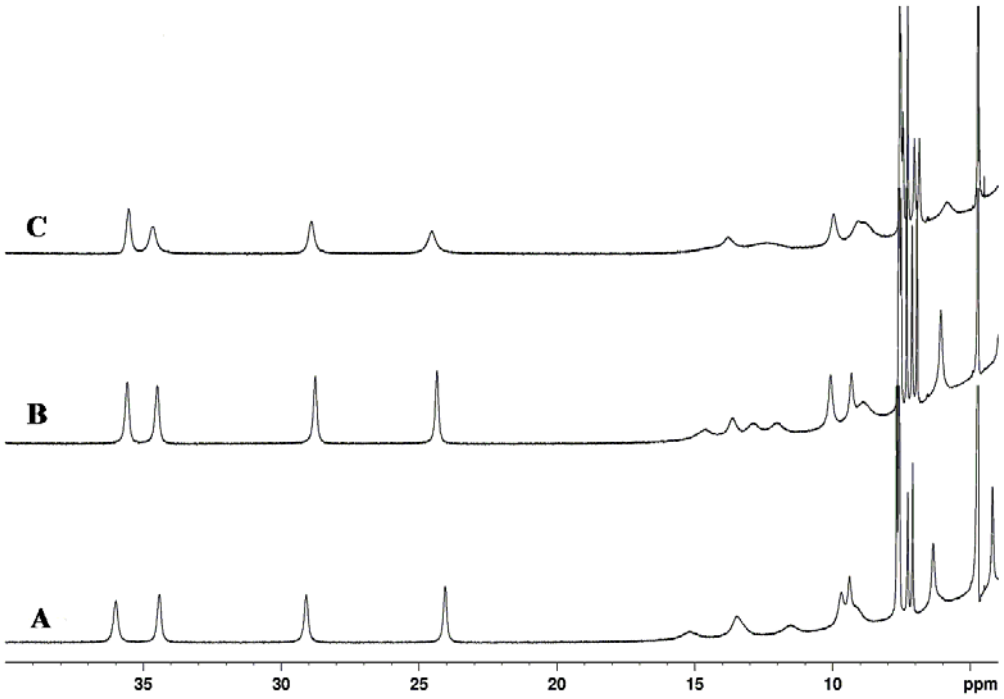

Figure S6. ^{1}H-NMR spectra of Eu(An-HP-DO3A) complex at pD=4.78 (**A**), 7.68 (**B**) and 9.33 (**C**) ([EuL]=2.0 mM, 14.1 T, D_2O, 278 K)

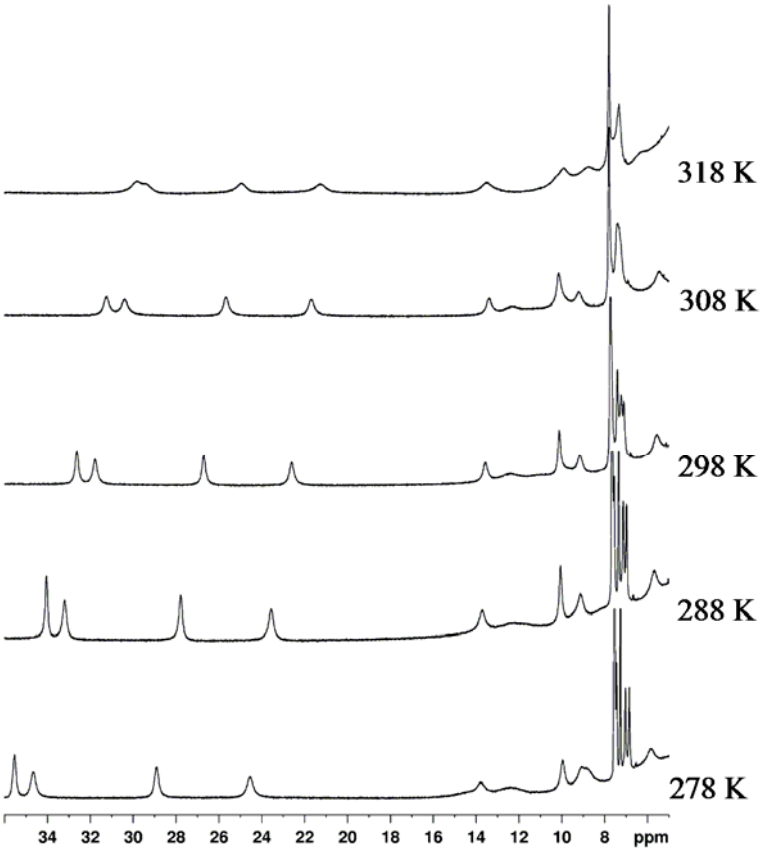

Figure S7. VT ^{1}H-NMR spectra of Eu(An-HP-DO3A) complex ([EuL]=2.5 mM, pD=7.68, 14.1 T, D_2O)

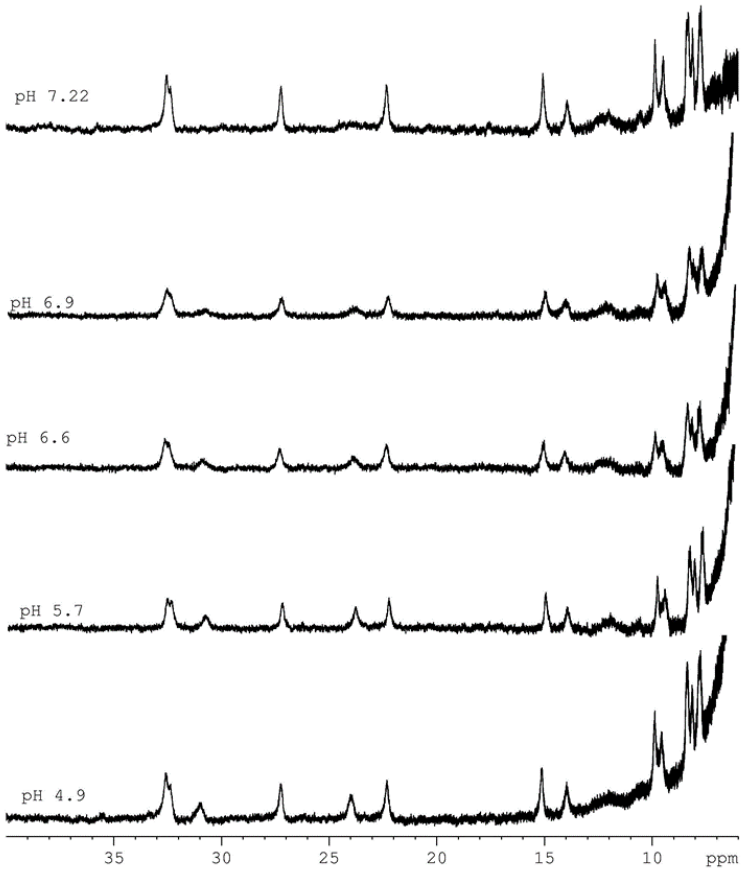

Figure S8. ^{1}H-NMR spectra of Eu(Bz-HP-DO3A) complex ([EuL]=17.1 mM, 14.1 T, H_2O, 298 K)

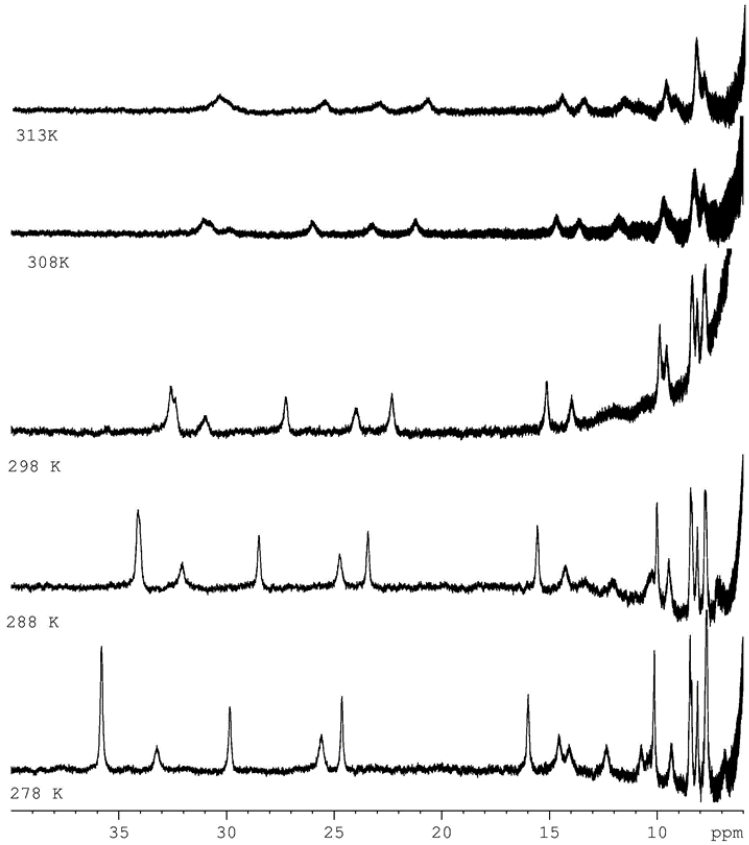

Figure S9. VT ^{1}H-NMR spectra of Eu(Bz-HP-DO3A) complex ([EuL]=17.1 mM, pH=4.9, 14.1 T, H_2O)

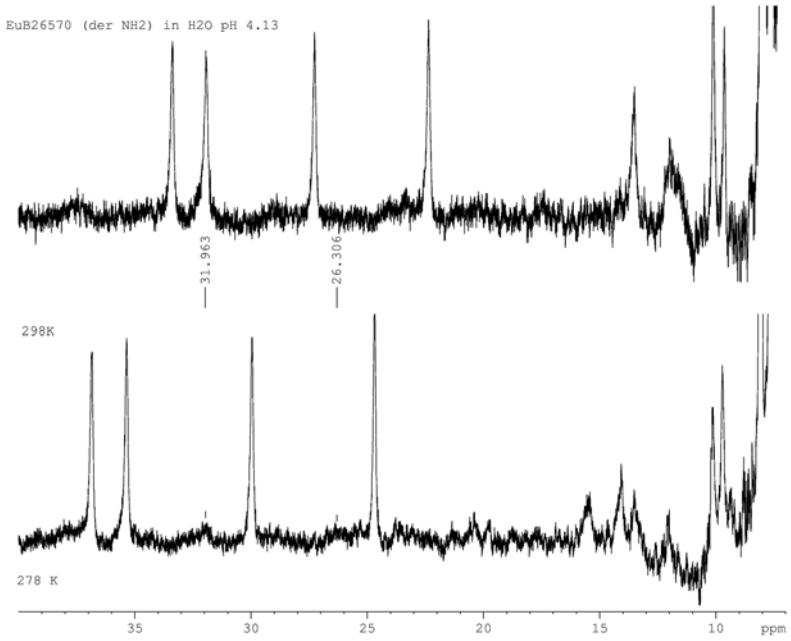

Figure S10. ^{1}H-NMR spectra of Eu(An-HP-DO3A) complex ([EuL]=15 mM, pH=4.13, 14.1 T, H_2O)

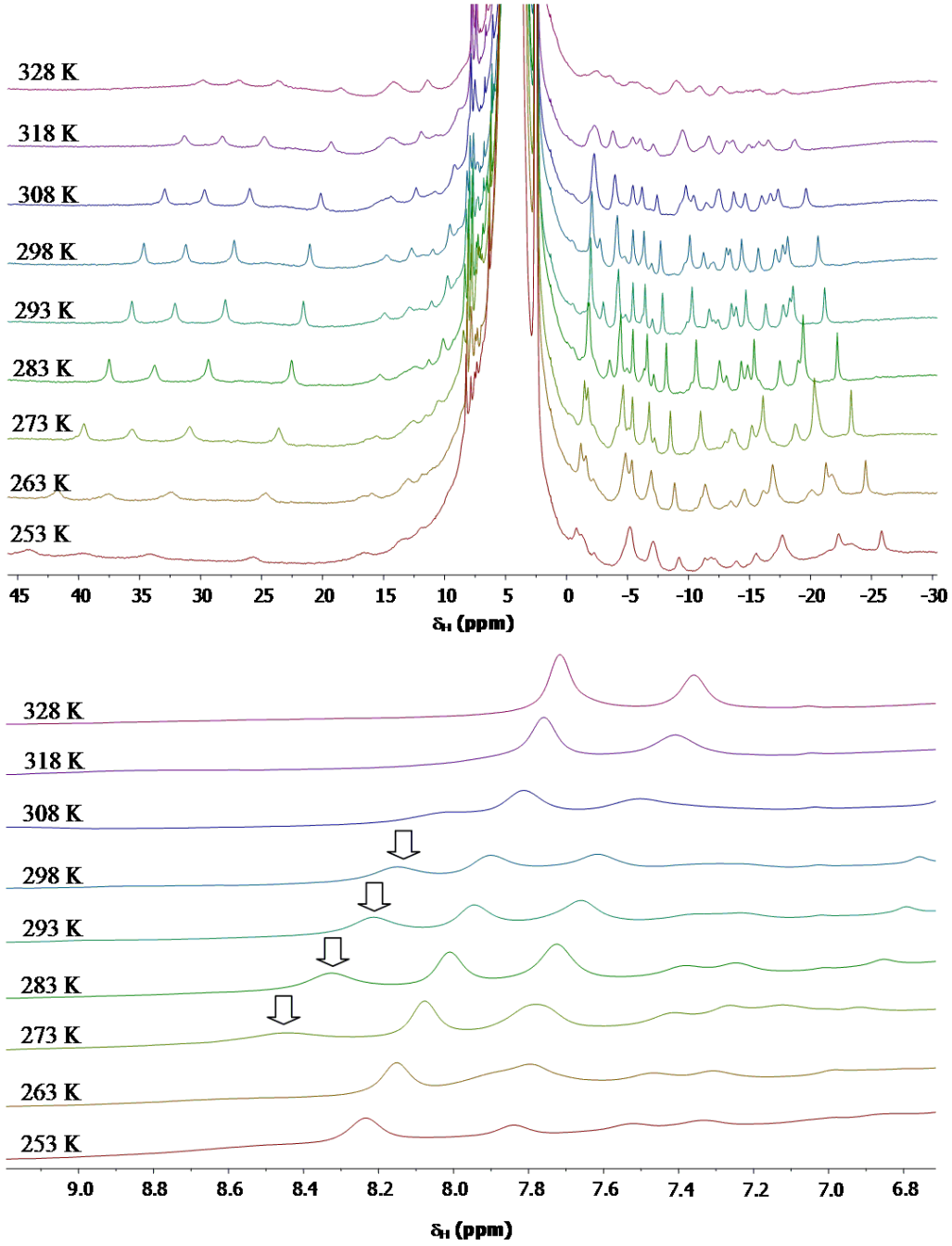

Figure S11. ^{1}H-NMR spectra of Eu-An-HP-DO3A)in 80/20 v/v% DMSO-d_6/H_2O mixture ([EuL]=0.05 M, pH=5.0, 11.4 T)

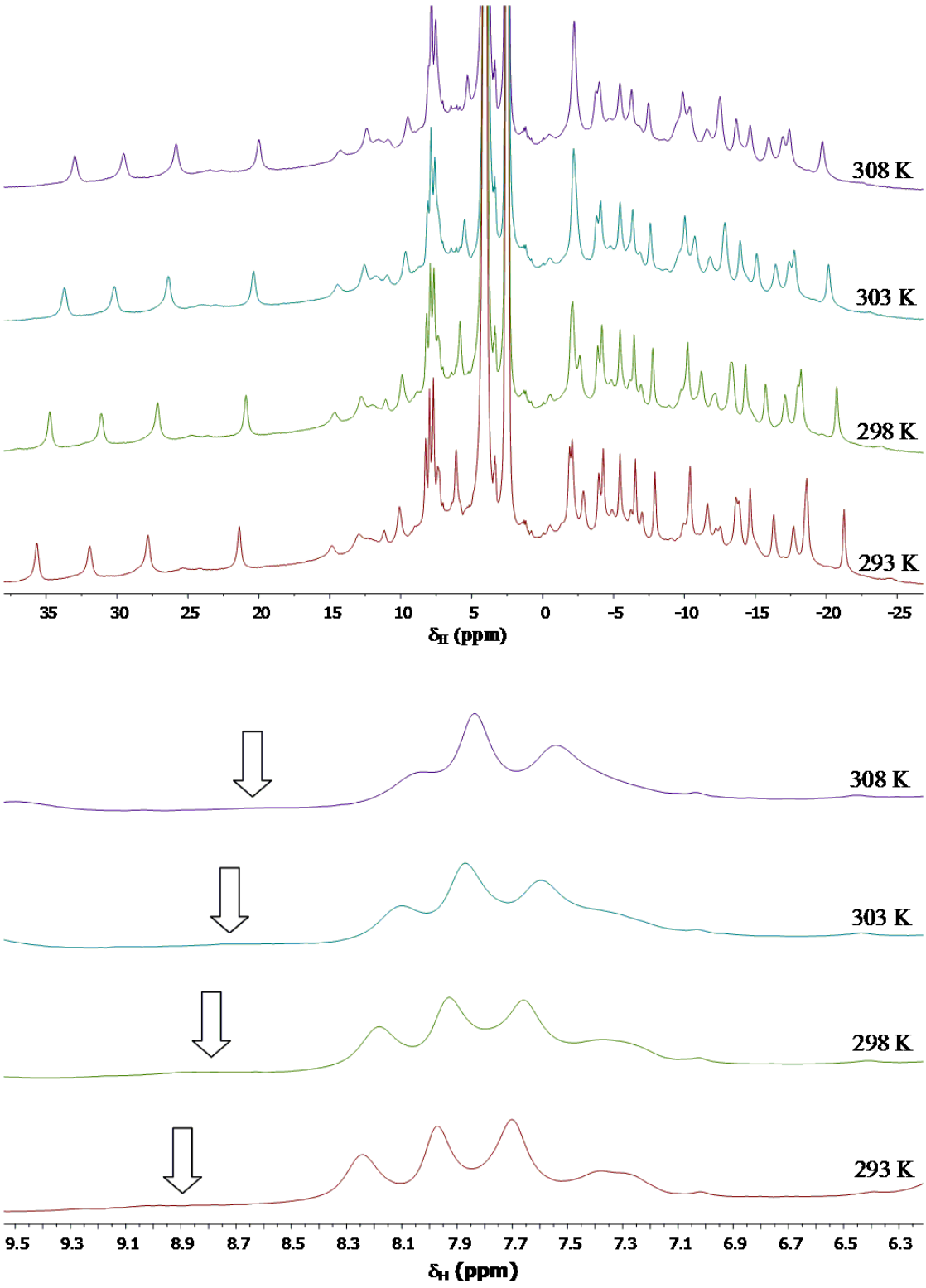

Figure S12. VT ^{1}H-NMR spectra of Eu(An-HP-DO3A) in 80/20 v/v% DMSO-d_6/D_2O mixture ([EuL]=0.05 M, pD=5.4, 9.4 T)

II. X-ray diffraction studies of Gd(Bz-HP-DO3A) and Gd(An-HP-DO3A)

Slow evaporation of concentrated H_2O solutions of the Gd(An-HP-DO3A) and Gd(Bz-HP-DO3A) complexes yielded single crystals of formula $[Gd(An\text{-}HP\text{-}DO3A)(H_2O)]_2 \cdot 12H_2O$ and $Na_2[Gd(Bz\text{-}HP\text{-}DO3A)(H_2O)]_2 \cdot 19H_2O$ suitable for analysis by single crystal X-ray diffraction studies. Data collections were performed at the XRD1 and XRD2 beamlines of the Elettra Synchrotron, Trieste (Italy)[S5]. The crystals were dipped in NHV oil (Jena Bioscience, Jena, Germany) and mounted on the goniometer head with kapton loops (MiTeGen, Ithaca, USA). Complete datasets were collected at 100 K (nitrogen stream supplied through an Oxford Cryostream 700) through the rotating crystal method. Data were acquired using monochromatic wavelengths of 0.700 Å or 0.620 Å on Pilatus hybrid-pixel area detectors (DECTRIS Ltd., Baden-Daettwil, Switzerland). The diffraction data were indexed, integrated and scaled using XDS.[S6] The structures were solved by the dual space algorithm implemented in the SHELXT code.[S7] Fourier analysis and refinement were performed by the full-matrix least-squares methods based on F^2 implemented in SHELXL (Version 2018/3).[S8] The Coot program was used for modeling.[S9] Anisotropic thermal motion refinement have been used for Gd^{III} ion in the cases of all complexes. Solvent molecules have been refined anisotropically for residues with occupancies greater than 50%. Limited geometry and thermal motion parameters restrains (DFIX, DANG, SIMU and DELU) have been used on disordered fragments with poor electron densities. Hydrogen atoms were included at calculated positions with isotropic $U_{factors} = 1.2 \cdot U_{eq}$ or $U_{factors} = 1.5 \cdot U_{eq}$ for hydroxyl groups (U_{eq} being the equivalent isotropic thermal factor of the bonded non hydrogen atom). Hydrogen atoms have been places on water molecules when supported by electron density Fourier difference maps. Figures were prepared using Ortep-3[S10] and CCDC Mercury[S11] software. Essential crystal and refinement data are reported below (Table S1). Selected mean bond distances, angles and geometrical parameters of hydrogen bonds are summarized in Tables S2 – S5. Label of atoms coordinated by Gd^{III}-ion is shown in Figure S14. Atoms in tables always bear a residue number (e.g. a "_11" or "_21" appended to Gd or "_13" or "_23" appended to O, which represent a metal coordinated apical water molecule). Labels are complemented with "A/B" letter if a specific atom has been modelled in two alternative conformations; conformations with higher occupancies are always associated with "A" letter. CCDC 2053436 and 2053437 contain the supplementary crystallographic data for Gd(Bz-HP-DO3A) and Gd(An-HP-DO3A) complexes, respectively. Related files can be obtained free of charge from The Cambridge Crystallographic Data Centre via https://www.ccdc.cam.ac.uk/structures.

Compounds crystallize in centrosymmetric monoclinic crystal forms as racemates, with two Gd^{III}-complexes in the asymmetric units (ASU; Figure S13). The carboxylate group of Gd(Bz-HP-DO3A) is deprotonated at our crystallization condition and therefore it requires the presence of the Na^+ ion for each Gd^{III}-complex to obtain electroneutrality. Gd(An-HP-DO3A), is crystallized without counter ion in neutral form. Several solvent water molecules were found mainly in the

crystal channels. Contribution of diffuse disordered solvent in Gd(An-HP-DO3A) crystal packing voids couldn't be modeled and has been removed using PLATON-SQUEEZE[S12] routine (245 e^- /cell in a volume of 963 $Å^3$, corresponding to ~23 additional disordered water molecules which have been included in the reported crystal properties). Crystal packing for the three compounds show similar features: Gd^{III}-complexes in the asymmetric units are characterized by the same stereochemical configuration. Gd^{III}-complexes in the asymmetric unit are held together by strong hydrogen bonds involving hydroxyl groups and core HP-DO3A ligand carboxylates (average $d_{-(O1)H\cdots(O4)OC-}$ = 2.631(2) Å). Remaining carboxylate acceptors are involved in several additional hydrogen bonds mediated by water molecules (Tables S3 and S5). Polar contacts are therefore mainly responsible for crystal packing stabilization.

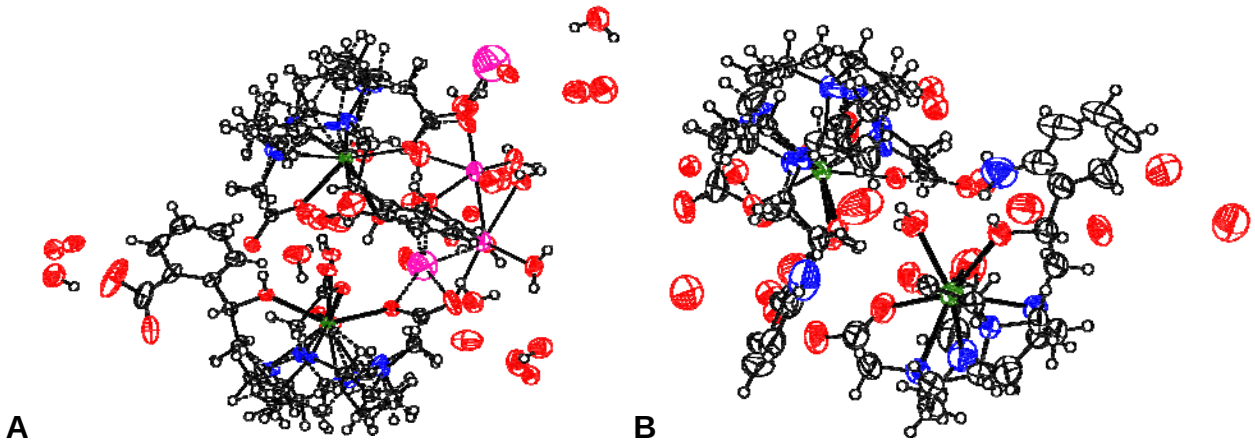

Figure S13. Ellipsoids representation (50% probability) of Gd(Bz-HP-DO3A) (A) and Gd(An-HP-DO3A) (B) crystallographic asymmetric unit contents (ASU).

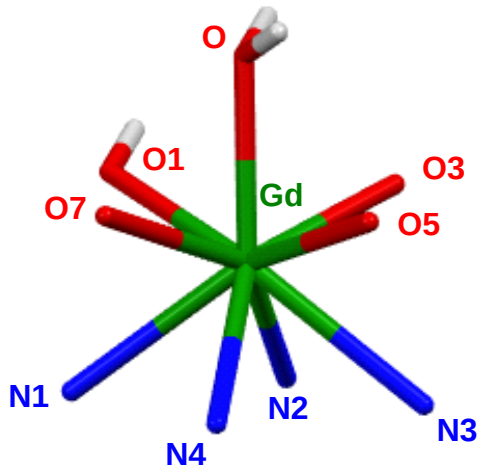

Figure S14. Label of atoms coordinated by Gd^{III}-ion in Gd(An-HP-DO3A) and Gd(Bz-HP-DO3A) complexes. Color code: Gd (green), O (red), N (blue) and H (grey).

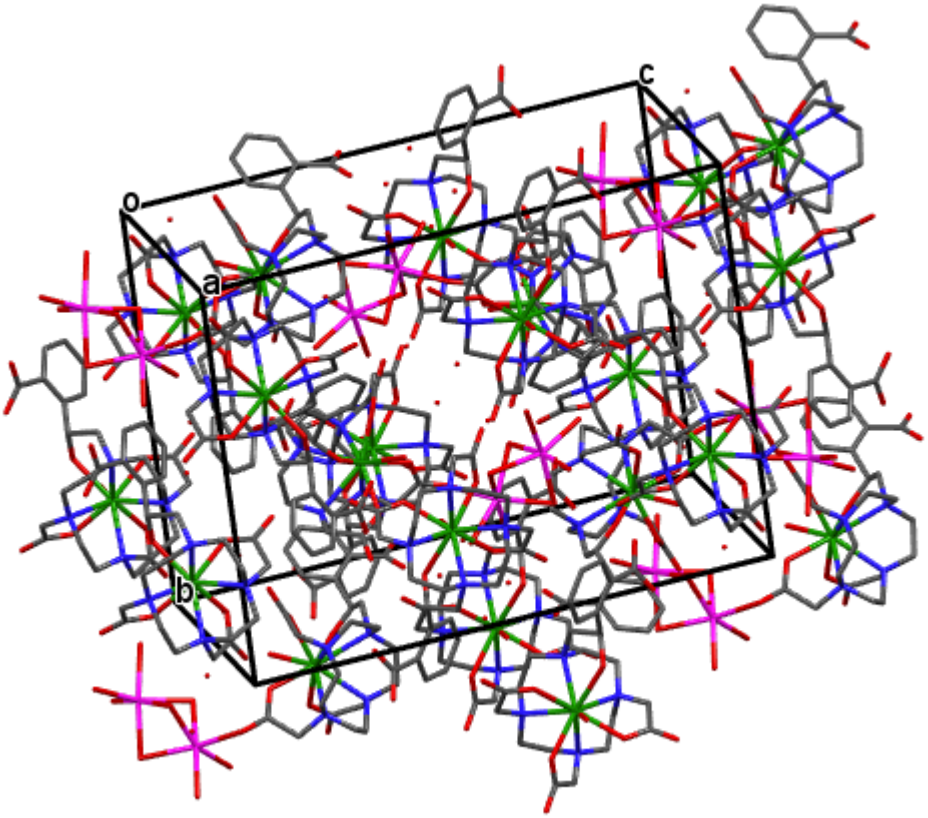

Figure S15. Packing diagram of $Na_2[Gd(Bz\text{-}HP\text{-}DO3A)(H_2O)]_2 \cdot 19H_2O$

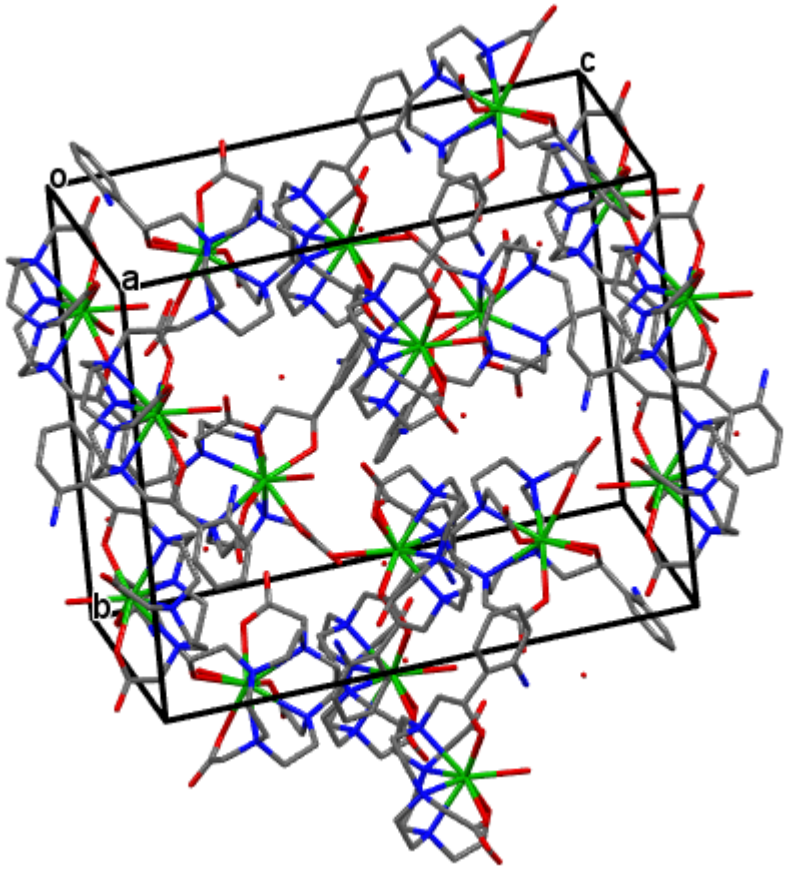

Figure S16. Packing diagram of $[Gd(An\text{-}HP\text{-}DO3A)(H_2O)]_2 \cdot 12H_2O$

Table S1. Crystallographic data and refinement details for Gd(Bz-HP-DO3A) and Gd(An-HP-DO3A).

	Gd(Bz-HP-DO3A)	**Gd(An-HP-DO3A)**
CCDC Number	2053436	2053437
Chemical Formula	$C_{23}H_{32}GdN_4O_{10}Na{\cdot}10.5(H_2O)$	$C_{22}H_{34}GdN_5O_8{\cdot}7(H_2O)$
Formula weight	893.93 g/mol	779.90 g/mol
Temperature	100(2) K	100(2) K
Wavelength	0.700 Å	0.620 Å
Crystal system	Monoclinic	Monoclinic
Space Group	$P\,2_1/c$	$P\,2_1/c$
Unit cell dimensions	a = 17.550(4) Å	a = 18.237(4) Å
	b = 17.234(3) Å	b = 17.179(3) Å
	c = 24.922(5) Å	c = 23.059(5) Å
	α = 90°	α = 90°
	β = 106.01(3)°	β = 107.97(3)°
	γ = 90°	γ = 90°
Volume	7245(3) Å^3	6872(3) Å^3
Z	8	8
Density (calculated)	1.639 g·cm^{-3}	1.508 g·cm^{-3}
Absorption coefficient	1.844 mm^{-1}	1.392 mm^{-1}
F(000)	3664	3192
Resolution	0.70 Å	0.62 Å
Theta range for data collection	2.0° to 30.0°	1.0° to 29.7°
Index ranges	$-25 \le h \le 25$, $-24 \le k \le 24$, $-35 \le l \le 35$	$-29 \le h \le 29$, $-27 \le k \le 26$, $-33 \le l \le 36$
Reflections collected	111879	121338
Independent reflections	22004, 21919 data with I>2σ(I)	29223, 19071 data with I>2σ(I)
Data multiplicity (max resltn)	5.00 (4.81)	4.06 (3.62)
I/σ(I) (max resltn)	69.74 (54.43)	15.55 (2.94)
R_{merge} (max resltn)	0.0263 (0.0352)	0.0438 (0.3321)
Data completeness (max resltn)	99.6% (99.8%)	99.1% (98.1%)
Refinement method	Full-matrix least-squares on F^2	Full-matrix least-squares on F^2
Data / restraints / parameters	22004 / 144 / 1268	29223 / 102 / 908
Goodness-of-fit on F^2	1.042	1.039
Δ/σ_{max}	0.013	0.004
Final R indices [I>2σ(I)]	R_1 = 0.0275, wR_2 = 0.0754	R_1 = 0.0626, wR_2 = 0.1849
R indices (all data)	R_1 = 0.0283, wR_2 = 0.0756	R_1 = 0.0918, wR_2 = 0.2079
Largest diff. peak and hole	1.215 and -1.468 eÅ^{-3}	2.742 and -3.019 eÅ^{-3}
R.M.S. deviation from mean	0.122 eÅ^{-3}	0.142 eÅ^{-3}

$$R_1 = \Sigma \, ||F_O|-|F_C|| \, / \, \Sigma \, |F_O|, \; wR_2 = \{\Sigma \, [w(F_O^2 - F_C^2)^2] \, / \, \Sigma \, [w(F_O^2)^2]\}^{½}$$

Table S2. Selected mean bond distances and angles (Å and °) for donor atoms coordinated by Gd^{III}-ion Gd(An-HP-DO3A). Label of atoms is reported in Figure S14.

Distances		(Å)		Angles			(°)	Angles			(°)
Gd_x1	O_x3	2.432(4)		O_x3	Gd_x1	O1_x2	68.80(12)	O3_x2	Gd_x1	N1_x2	126.32(21)
Gd_x1	O1_x2	2.445(3)		O_x3	Gd_x1	O3_x2	69.71(11)	O3_x2	Gd_x1	N2_x2	64.88(18)
Gd_x1	O3(A/B)_x2	2.396(3)		O_x3	Gd_x1	O5_x2	73.68(13)	O3_x2	Gd_x1	N3_x2	77.47(20)
Gd_x1	O5(A/B)_x2	2.349(5)		O_x3	Gd_x1	O7_x2	71.72(13)	O3_x2	Gd_x1	N4_x2	144.05(25)
Gd_x1	O7(A/B)_x2	2.342(3)		O_x3	Gd_x1	N1_x2	127.20(20)	O5_x2	Gd_x1	N1_x2	146.74(21)
Gd_x1	N1(A/B)_x2	2.642(10)		O_x3	Gd_x1	N2_x2	124.73(22)	O5_x2	Gd_x1	N2_x2	126.53(19)
Gd_x1	N2(A/B)_x2	2.669(8)		O_x3	Gd_x1	N3_x2	129.29(22)	O5_x2	Gd_x1	N3_x2	65.00(26)
Gd_x1	N3(A/B)_x2	2.679(9)		O_x3	Gd_x1	N4_x2	131.92(26)	O5_x2	Gd_x1	N4_x2	79.05(26)
Gd_x1	N4(A/B)_x2	2.632(10)		O1_x2	Gd_x1	O3_x2	86.38(10)	O7_x2	Gd_x1	N1_x2	80.74(25)
				O1_x2	Gd_x1	O5_x2	142.38(13)	O7_x2	Gd_x1	N2_x2	146.53(20)
				O1_x2	Gd_x1	O7_x2	82.64(12)	O7_x2	Gd_x1	N3_x2	127.63(21)
				O3_x2	Gd_x1	O5_x2	82.68(12)	O7_x2	Gd_x1	N4_x2	66.83(26)
				O3_x2	Gd_x1	O7_x2	141.30(12)	N1_x2	Gd_x1	N2_x2	66.53(28)
				O5_x2	Gd_x1	O7_x2	83.83(14)	N1_x2	Gd_x1	N3_x2	103.23(29)
				O1_x2	Gd_x1	N1_x2	63.75(20)	N1_x2	Gd_x1	N4_x2	68.33(30)
				O1_x2	Gd_x1	N2_x2	78.99(21)	N2_x2	Gd_x1	N3_x2	67.52(28)
				O1_x2	Gd_x1	N3_x2	146.23(22)	N2_x2	Gd_x1	N4_x2	103.25(29)
				O1_x2	Gd_x1	N4_x2	125.96(25)	N3_x2	Gd_x1	N4_x2	66.88(30)

Table S3. Geometrical parameters of hydrogen bonds found in the crystal packing of Gd(An-HP-DO3A). Label of atoms is reported in Figure S14.

D-H···A	d(D-H) (Å)	d(H···A) (Å)	d(D···A) (Å)	<(DHA) (°)
O1_12-H1_12···O4A_22^a	0.84	1.91	2.734(4)	167.1
O1_22-H1_22^a···O4_12	0.84	1.74	2.584(4)	176.9
C11_12-H11A_12···O_32	0.99	2.66	3.582(8)	155.8
C10_12-H10B_12···O6A_22^a#10.99	2.62	3.474(8)	145.2	
C10_12-H10B_12···OC_37^c#1	0.99	2.64	3.251(15)	120.0
C9_12-H9A_12···OB_37^b#1	0.99	2.54	3.297(12)	133.2
C13_12-H13A_12···O6A_22^a#10.99	2.43	3.309(8)	147.3	
C15_12-H15B_12···O6_12#2	0.99	2.51	3.429(8)	153.4
C17_12-H17B_12···O6_12#2	0.99	2.48	3.355(8)	147.4
C22_12-H22B_12···OA_40#3	0.99	2.63	3.614(18)	172.3
C1_12-H1A_12···O7_12	0.99	2.55	3.130(8)	117.0
C2_12-H2_12···OA_37^a	1.00	2.53	3.497(9)	161.8
NA_12-HA1_12···OA_40	0.88	2.24	2.786(18)	120.4
NA_12-HA2_12···O7_12	0.88	2.41	3.061(9)	131.4
NA_12-HA2_12···O1_12	0.88	2.26	2.895(8)	129.1
NA_12-HA2_12···O_13	0.88	2.55	3.326(8)	147.9
O_13-H1_13···O3A_22^a	0.87	2.06(3)	2.866(5)	153(6)
O_13-H2_13···O_33	0.87	1.91(3)	2.742(8)	159(7)
C13A_22^a-H13B_22^a···O8A_22^a#4	0.99	2.52	3.392(10)	146.3
C18A_22^a-H18B_22^a···O_34#50.99	2.60	3.222(10)	120.9	
C19A_22^a-H19B_22^a···OA_37^a#6	0.99	2.64	3.341(14)	128.3
C21A_22^a-H21B_22^a···O4A_22^a#5	0.99	2.62	3.362(6)	132.0
C22A_22^a-H22B_22^a···OA_38^a#5	0.99	2.64	3.615(16)	166.5
C1A_22^a-H1A_22^a···O7A_22^a0.99	2.65	3.315(13)	125.0	
C13B_22^b-H13C_22^b···O8B_22^b#4	0.99	2.17	3.143(19)	167.5
C14B_22^b-H14D_22^b···O3B_22^b	0.99	2.49	3.07(3)	117.2
C18B_22^b-H18C_22^b···O_34#50.99	2.40	3.27(2)	146.4	
C1B_22^b-H1B1_22^b···O7B_22^b	0.99	2.58	3.22(5)	122.5
NA_22-HA1_22···O4_12#7	0.88	2.17	3.024(7)	162.1
O_23-H1_23···OA_39^a	0.87	2.15(6)	2.707(16)	122(5)
O_23-H1_23···OB_39^b	0.87	2.10(5)	2.834(14)	141(6)
O_23-H2_23···O3_12	0.87	1.97(2)	2.805(4)	163(7)

Symmetry transformations used to generate equivalent atoms:
#1 x,-y+3/2,z+1/2; #2 -x+2,-y+1,-z+1; #3 -x+2,-y+2,-z+1; #4 -x+1,y+1/2,-z+1/2; #5 -x+1,y-1/2,-z+1/2
#6 x,-y+3/2,z-1/2; #7 -x+1,-y+1,-z+1

Table S4. Selected mean bond distances and angles (Å and °) for donor atoms coordinated by Gd^{III}-ion Gd(Bz-HP-DO3A). Label of atoms is reported in Figure S14.

Distances		(Å)		Angles			(°)	Angles			(°)
Gd_x1	O_x3	2.440(2)		O_x3	Gd_x1	O1_x2	69.55(6)	O3_x2	Gd_x1	N1_x2	125.02(9)
Gd_x1	O1_x2	2.413(2)		O_x3	Gd_x1	O3_x2	69.46(5)	O3_x2	Gd_x1	N2_x2	64.73(8)
Gd_x1	O3_x2	2.403(2)		O_x3	Gd_x1	O5_x2	72.55(6)	O3_x2	Gd_x1	N3_x2	79.60(8)
Gd_x1	O5_x2	2.366(2)		O_x3	Gd_x1	O7_x2	71.87(6)	O3_x2	Gd_x1	N4_x2	146.30(12)
Gd_x1	O7(A/B)_x2	2.360(2)		O_x3	Gd_x1	N1_x2	127.86(8)	O5_x2	Gd_x1	N1_x2	146.61(9)
Gd_x1	N1(A/B)_x2	2.655(6)		O_x3	Gd_x1	N2_x2	126.59(8)	O5_x2	Gd_x1	N2_x2	126.31(8)
Gd_x1	N2(A/B)_x2	2.667(6)		O_x3	Gd_x1	N3_x2	128.46(7)	O5_x2	Gd_x1	N3_x2	64.71(11)
Gd_x1	N3(A/B)_x2	2.667(5)		O_x3	Gd_x1	N4_x2	130.44(7)	O5_x2	Gd_x1	N4_x2	78.86(8)
Gd_x1	N4(A/B)_x2	2.645(6)		O1_x2	Gd_x1	O3_x2	84.07(6)	O7_x2	Gd_x1	N1_x2	80.90(8)
				O1_x2	Gd_x1	O5_x2	141.98(6)	O7_x2	Gd_x1	N2_x2	147.16(8)
				O1_x2	Gd_x1	O7_x2	83.62(6)	O7_x2	Gd_x1	N3_x2	126.02(8)
				O3_x2	Gd_x1	O5_x2	84.82(6)	O7_x2	Gd_x1	N4_x2	65.45(12)
				O3_x2	Gd_x1	O7_x2	141.31(6)	N1_x2	Gd_x1	N2_x2	66.72(10)
				O5_x2	Gd_x1	O7_x2	82.76(6)	N1_x2	Gd_x1	N3_x2	103.59(10)
				O1_x2	Gd_x1	N1_x2	64.14(9)	N1_x2	Gd_x1	N4_x2	68.20(6)
				O1_x2	Gd_x1	N2_x2	80.10(8)	N2_x2	Gd_x1	N3_x2	67.30(10)
				O1_x2	Gd_x1	N3_x2	146.87(8)	N2_x2	Gd_x1	N4_x2	102.96(10)
				O1_x2	Gd_x1	N4_x2	125.92(13)	N3_x2	Gd_x1	N4_x2	67.17(10)

Table S5. Geometrical parameters of hydrogen bonds found in in the crystal packing of Gd(Bz-HP-DO3A). Label of atoms is reported in Figure S14.

D-H···A	d(D-H) (Å)	d(H···A) (Å)	d(D···A) (Å)	<(DHA) (°)
O1_12-H1_12···O4_22	0.84	1.86	2.681(2)	164.0
O1_22-H1_22···O4_12	0.84	1.73	2.558(2)	165.8
C2_12-H2_12^a···OA_12	1.00	2.16	2.935(3)	132.8
C21A_12^a-H21A_12^a···O_61#20.99	2.49	3.390(5)	150.3	
C11A_12^a-H11A_12^a···OA_15^a#3	0.99	2.45	3.430(3)	169.1
C17A_12^a-H17B_12^a···O6_12#4	0.99	2.41	3.388(4)	168.4
C9A_12^a-H9A1_12^a···O_61#20.99	2.62	3.600(6)	169.4	
C1A_12^a-H1A1_12^a···O8A_12^a#1	0.99	2.56	3.475(4)	153.8
C14A_12^a-H14A_12^a···O3_120.99	2.65	3.130(4)	110.1	
C13A_12^a-H13A_12^a···OA_59^a#2	0.99	2.46	3.060(4)	118.8
C22B_12^b-H22C_12^b···OB_52^b#1	0.99	2.50	3.353(13)	144.4
C22B_12^b-H22D_12^b···O_61#20.99	2.49	3.455(8)	164.5	
C18B_12^b-H18D_12^b···O_61#20.99	2.60	3.582(7)	169.3	
C1B_12^b-H1B2_12^b···O7B_12^b	0.99	2.53	3.245(3)	128.7
C19B_12^b-H19D_12^b···O5_120.99	2.66	3.209(3)	115.6	
C14B_12^b-H14D_12^b···OB_59^b#2	0.99	2.65	3.131(8)	110.0
C13B_12^b-H13D_12^b···OB_56^b#3	0.99	2.50	3.30(2)	137.1
C15B_12^b-H15C_12^b···O3_120.99	2.60	3.252(3)	123.7	
O_13-H1_13···O3_22	0.87	1.930(6)	2.797(2)	177(3)
O_13-H2_13···OA_47^a	0.87	1.839(10)	2.692(2)	166(3)
O_13-H2_13···OB_47^b	0.87	2.445(18)	3.303(17)	169(3)
C2_22-H2_22^a···OA_22	1.00	2.36	2.896(3)	112.5
C1A_22^a-H1A1_22^a···O_53#50.99	2.65	3.556(3)	153.0	
C1A_22^a-H1A2_22^a···O7_22	0.99	2.62	3.316(3)	127.1
C9A_22^a-H9A2_22^a···O_48#30.99	2.59	3.228(3)	121.9	
C1B_22^b-H1B1_22^b···O_53#50.99	2.59	3.556(3)	165.8	
C9B_22^b-H9B2_22^b···O_53#50.99	2.56	3.522(10)	164.4	
C18B_22^b-H18C_22^b···O5_220.99	2.57	3.070(12)	110.9	
C18B_22^b-H18D_22^b···OB_59^b#6	0.99	2.43	3.318(11)	149.3
O_23-H1_23···OA_51^a	0.87	1.96(2)	2.743(3)	149(4)
O_23-H1_23···OB_51^b	0.87	2.03(2)	2.873(16)	164(3)
O_23-H2_23···O3_12	0.87	2.022(6)	2.890(2)	176(4)
O_41-H2_41···O5_12	0.87	2.098(15)	2.922(3)	158(3)
O_42-H1_42···O4_12#7	0.87	2.065(12)	2.913(3)	164(3)
O_42-H2_42···OA_52^a	0.87	2.011(15)	2.828(4)	156(3)

O_43-H2_43···O8_22#8	0.87	2.18(3)	2.895(3)	140(3)
O_44-H1_44···OA_62^a	0. 87	2.03(3)	2.742(6)	137(4)
O_45-H1_45···O_55#9	0. 87	2.22(4)	2.890(5)	133(4)
O_46-H1_46···OA_12#7	0. 87	1.938(7)	2.807(3)	176(4)
O_46-H2_46···O4_22#7	0.87	1.904(11)	2.759(3)	167(4)
O_48-H1_48···OA_22#7	0.87	2.137(17)	2.941(3)	153(3)
O_48-H2_48···O_58	0.87	2.10(2)	2.896(4)	151(4)
O_53-H1_53···OA_47^a	0.87	1.985(19)	2.804(3)	156(4)
O_53-H1_53···OB_47^b	0.87	2.60(3)	3.324(17)	141(3)
O_53-H2_53···O_58#10	0.87	1.889(7)	2.758(4)	175(4)
O_54-H1_54···O8_22	0. 87	1.973(16)	2.815(3)	162(4)
O_54-H2_54···OA_60^a#8	0.87	2.235(19)	3.069(10)	160(4)
O_54-H2_54···OB_60^b#8	0.87	1.844(15)	2.701(8)	168(5)
O_55-H1_55···OA_12#1	0. 87	2.30(3)	2.782(4)	115(3)
O_55-H2_55···OB_56^b	0. 87	1.99(3)	2.64(2)	130(3)
O_58-H1_58···OA_22#6	0.87	1.927(11)	2.787(4)	169(5)
O_58-H2_58···OA_60^a	0.87	1.867(10)	2.735(7)	175(5)
O_58-H2_58···OB_60^b	0.87	2.13(2)	2.963(7)	159(5)
O_61-H1_61···OA_59^a	0.87	1.751(16)	2.607(5)	168(7)
O_61-H1_61···OB_59^b	0.87	2.231(17)	3.072(8)	163(5)
O_61-H2_61···OA2_22	0.87	2.02(4)	2.753(6)	141(6)

Symmetry transformations used to generate equivalent atoms:
#1 -x+2,-y+2,-z+1; #2 -x+2,y+1/2,-z+1/2; #3 x,-y+3/2,z-1/2; #4 -x+2,-y+1,-z+1; #5 -x+1,y-1/2,-z+1/2
#6 -x+1,y+1/2,-z+1/2; #7 x,-y+3/2,z+1/2; #8 -x+1,-y+1,-z+1; #9 -x+2,y-1/2,-z+3/2; #10 -x+1,-y+2,-z+1

III. References

[S1] I. M. Carnovale, M. L. Lolli, S. Colombo Serra, A. Fringuello Mingo, R. Napolitano, V. Boi, N. Guidolin, L. Lattuada, F. Tedoldi, Z. Baranyai, S. Aime, *Chem. Commun.* 2018, **54**, 10056-10059.

[S2] D. M. Corsi, C. Platas-Iglesias, H. van Bekkum and J. A. Peters, *Magn. Reson. Chem.* 2001, **39**, 723–726.

[S3] J. Stancanello, E. Terreno, D. D. Castelli, C. Cabella, F. Uggeri, S. Aime S. *Cont. Med. Mol. Imag.*, 2008, **4**, 136–149.

[S4] E. Terreno, J. Stancanello, D. L. Longo, D. D. Castelli, L. Milone, H. M. Sanders, M. B. Kok, F. Uggeri, S. Aime, *Cont. Med. Mol. Imag.*, 2009, **4**, 237.

[S5] A. Lausi, M. Polentarutti, S. Onesti, J. R. Plaisier, E. Busetto, G. Bais, L. Barba, A. Cassetta, G. Campi, D. Lamba, A. Pifferi, S. C. Mande, D. D. Sarma, S. M. Sharma, G. Paolucci, *Eur. Phys. J. Plus*, 2015, **130**, 1-8.

[S6] W. Kabsch, *Acta Cryst.*, 2010, **D66**(2), 125–132.

[S7] G. M. Sheldrick, *Acta Cryst.*, 2015, **A71**, 3-8.

[S8] G. M. Sheldrick, *Acta Cryst.*, 2015, **C71**, 3-8.

[S9] P. Emsley, B. Lohkamp, W. G. Scott, K. Cowtan, Acta Cryst. 2010, **D66**(4), 486–501.

[S10] L. J. Farrugia, *J. Appl. Cryst.*, 2012, **45**, 849-854.

[S11] C. F. Macrae, I. J. Bruno, J. A. Chisholm, P. R. Edgington, P. McCabe, E. Pidcock, L. Rodriguez-Monge, R. Taylor, J. van de Streek, P. A. Wood. 2008. *J. Appl. Cryst.*, **41**, 466-470.

[S12] A. Spek, *Acta Cryst*, 2015, **C71**, 9-18.